Available online at http://scik.org

J. Math. Comput. Sci. 11 (2021), No. 6, 7487-7510

https://doi.org/10.28919/jmcs/6571

ISSN: 1927-5307

INTERPOLATION METHOD FOR EVALUATING WEAKLY SINGULAR KERNELS

E. S. SHOUKRALLA*

Department of Engineering Mathematics and Physics, Faculty of Electronic Engineering, Menoufia University, Egypt

Abstract: The solution of initial, boundary, and mixed value problems through the integral equation method yields certain boundary singular integral equations. In many scientific and industrial applications in artificial intelligence, biological systems, scattering, radiation, and image processing, there is a need to evaluate such types of singular integrals, especially the weakly singular kernels. This study presents a new numerical method for evaluating weakly singular kernels based on some advanced matrix-vector barycentric Lagrange interpolation formulas. We developed these formulas to be applied to numerically evaluating singular integrals. At the same time, we created three computational rules to determine the optimal locations for the distribution of the interpolation nodes to be within the integration domain and never be outside for any value of the interpolant degree. These rules are devised so that the equidistant nodes depend on the step-sizes, which are defined as functions of the interpolant degree by some small real number greater than or equal to zero. Thus, we overcame the singularity of the kernels on the whole integration domain and obtained uniform interpolation. Moreover, the presented method gives the kernel's values and the kernel's integral values at the singular points, whereas the numerical or exact values do not exist. The solutions to the illustrated four examples are shown in the given tables and figures. The interpolant solutions which we obtain by low-degree interpolants are faster to converge to the numerical or exact ones (if they exist). This confirms the originality of the presented method and its effectiveness in obtaining high-precision results.

Keywords: barycentric Lagrange interpolation; singular integral; weakly singular Fredholm kernels; computational methods; biological systems; scattering, radiation; image processing.

2010 AMS Subject Classification: 45D05, 65R20.

*Corresponding author

E-mail address: shoukralla@el-eng.menofia.edu.eg

Received July 28, 2021

1. INTRODUCTION

The need to use the concept of interpolating functions is more urgent than ever before, especially after the progress that has happened in the development of biological systems science, environmental engineering, virology, and epidemiology and their impact on public health, since these applications rely on processing data mathematically and converting it into interpolant polynomials [1-4]. Oftentimes, researchers need to deal with interpolating polynomials via matrices rather than the polynomial forms. This greatly contributes to evaluating singular integrals more easily than by using the usual methods. The reason for this is that it is easy to separate the integration variables from polynomials and construct what is called the monomial basis matrix. Then it is easier to integrate only the monomial functions than to integrate the polynomials themselves.

One of the most famous interpolations is the barycentric Lagrange interpolation [5-6]. Shoukralla et. al. [7-11] modified the barycentric Lagrange interpolation formula and obtained advanced matrix-vector barycentric interpolation formulas, which were applied to solve non-singular linear Volterra integral equations of the second kind. The solution of weakly singular integral equations is more difficult due to the singularity of the unknown functions and the kernels. Shoukralla et. al. [12-14] provide methods for the solution of such singular equations based on orthogonal functions with the analytical treatment of the kernel singularity. The mathematical treatment of the kernel singularity adopted in these methods was difficult and complicated. Additionally, there are many papers that have been published to evaluate singular integrals, but they are also not as easy as required and rely on more complicated techniques. [15-18]. Based on the specified asymptotic analysis, Jing Gao et al. [15], constructed a Filon-type method to approximate similar-type integrals which achieved high accuracy for both small and large frequencies. This method ensures the interpolation at the zeros of polynomials orthogonal to a complex weight function. Andrei K. Lerner [16], obtained a certain weak type estimate for maximal operators related to some classes of classical rough homogeneous singular integrals. Benjamin Jaye et al. [17], presented a small local action notation condition subjected to a singular integral operator that is necessary for the existence of the principal value integral. Andrei K et al. [18], established the necessity for many classes of operators to provide new results even in the unweighted setting for first-order commutators. Thus, a Bloom-type characterization of the two-weighted boundedness of iterated commutators of singular integrals is obtained. These aforementioned complications have pushed

us to search for new simple alternative methods that are easier, lead to accurate results, and can transform singular integrals into non-singular ones.

The presented study focuses on evaluating singular kernels based on the advanced barycentric Lagrange matrix-vector double interpolant formulas which were applied for solving non-singular integral equations [12-14]. The goal is not only to develop these formulas based on providing them with optimal node distribution rules, but also to make them capable of treating the singularities of the singular integrals and their evaluation with ease.

The rules for the equidistant node's distribution are established so that the coefficients of the square matrices of the barycentric functions never become singular matrices. Using these rules, we considered the step-sizes depending on a small number greater than zero, which we imposed as a function of the degree of the interpolant polynomial, so that the value of this small real number changes as the degree of the interpolant polynomial changes. This ensures that the nodes are fully distributed inside the integration domain and never be outside, and hence we get uniform interpolation. Also, the presented method is eligible to provide the kernel functional values at the endpoints of the integration domain, whereas the exact (or numerical) integral values of the kernels at the endpoints do not exist.

We concentrate on the weakly singular kernels of Fredholm integral equations of the second kind, which is usually given in the form $k(x,y)=|x-t|^{-\alpha}$; $0<\alpha<1$. The three established rules were created in such a way that the kernel denominator never approaches zero when $x \to t$. The interpolant integral values of the seven computed integrals in the four examples, as shown in the tables and graphs, strongly converge to the exact (or numerical) integral values in the integration domain. The obtained results ensure the originality and superiority of the presented method.

2. INTERPOLATION METHOD

We present a new method for evaluating weakly singular kernels of integral equations. The presented method is based on the modification of the matrix-vector interpolation formulas for non-singular integral equations to be suitable for evaluating singular kernels. Shoukralla et al. [12-14] reformulated the traditional barycentric Lagrange formula through matrices and thus were able to separate the coefficients of the barycentric functions from the monomial basis functions. Thus, they obtained an advanced formula consisting of the product of four matrices, one of which is the

matrix of monomials, to be applied to interpolating single-valued functions. They also obtained another formula for functions in two variables and expressed it through five matrices, two of which are monomial basis functions; each one is related to one variable. Furthermore, let $f(x)\in C^{n+1}[a,\mathrm{b}]$ and $f_n(x)$ be the matrix-vector barycentric Lagrange interpolating polynomial of degree n that interpolates $f(x)$ at the $(n+1)$ equidistant distinct nodes $\{x_i\}_{i=0}^{n}\subset[a,b]$, then $u_n(x)$ is expressed by [12]

$$f_n(x)=\mathrm{X}(x)\mathrm{CWF} \tag{1}$$

Here $\mathrm{F}=\left[f_i\right]_{i=0}^{n}$ is the $(n+1)\times 1$ column matrix such that the entries f_i satisfies the interpolation condition $f_n(x_i)=f_i$ for $i=\overline{0:n}$, $\mathrm{W}=diag\{w_i\}_{i=0}^{n}$ is a square diagonal matrix whose entries are defined by $w_i=(-1)^i\binom{n}{i}$, $\mathrm{X}(x)=\left[x^i\right]_{i=0}^{n}$ is the $1\times(n+1)$ monomial basis functions row matrix and $\mathrm{C}^T=\left[c_{ij}\right]_{i,j=0}^{n}$ is the $(n+1)\times(n+1)$ known Maclaurin coefficients matrix whose entries c_{ij} are defined by

$$c_{ij}=\frac{\psi_i^{(j)}(0)}{j!};\psi_i(x)=\frac{\zeta_i(x)}{\phi(x)},\phi(x)=\sum_{i=0}^{n}w_i\zeta_i(x),\ \zeta_i(x)=\frac{1}{x-x_i} \tag{2}$$

Where, we designed the rule of calculating the $x-$nodes distribution set $\{x_i\}_{i=0}^{n}$ by the formula

$$x_i=(a+\delta_1)+ih_1\ ;h_1=\frac{(b-\delta_1)-(a+\delta_1)}{n}\ ;\delta_1\geq 0,\ i=\overline{0,n} \tag{3}$$

Now, we focus on the interpolation of certain types of the two-variable valued functions which are defined on the triangle $\Gamma=\{(x,t);a\leq x,t\leq b\}$, where the integration will be held with respect to the only one variable t namely, t. We consider the weakly singular kernel of Fredholm integral equation of the second kind which often takes the form $k(x,t)=|x-t|^{-\alpha}$ where $0<\alpha<1$ and $a\leq x,t\leq b$. Let $\tilde{k}(x)=\int_a^b k(x,t)dt$, then $\tilde{k}(x)$ is singular integral when $x\to t$ under the assumption

that $\left|\int_a^b \frac{1}{|x-t|^{\alpha}} dt\right| \leq \varepsilon$ for some real number $\varepsilon \geq 0$ where $a \leq x \leq b$. As an inevitable consequence of the singularity of such kernels, when the variable x approaches the variable t, we follow the same steps as for the interpolation of $f(x)$ but with some fundamental differences. The first difference is that the domain of the definition of the kernel is the triangle Γ, and the second difference is related to the way that the nodes will be distributed inside the kernel domain Γ for both variables x and t, so that we ensure that $x > t$ and hence $k(x,t)$ never tends to infinity for any $n \geq 1$. We provide three rules (I), (II), and (III) for the equidistant nodes distributions for the two variables x and y such that the $t-$ nodes distributions depend on the $x-$ nodes distribution. These distributions are considering the optimal choice since they ensure that the magnitude $x-t$ never approaches zero, and thus we overcome the kernel's singularity. The realization of this ambition needs to define the step size h through a small number $\delta \geq 0$ which we establish as a function of the interpolant degree n. To obtain Rule (I), we interpolate $k(x,t)$ twice with different step-sizes for the two sets of equidistance interpolation nodes $\{x_i\}_{i=0}^{n}$ and $\{t_i\}_{i=0}^{n}$ corresponding to both variables x and t. After getting the matrix-vector barycentric matrix-vector double interpolant kernel $k_{n,n}(x,t)$, we integrate it with respect to the variable t to get $\tilde{k}_{n,n}(x)$. We choose the set of $x-$ nodes distributions $\{x_i\}_{i=0}^{n}$ as follows

$$x_i = (a+\delta) + ih \; ; h = (b-a-2\delta)/n \; ; \delta = 0, \text{or } \delta = (b-a)/\lambda(n+1), i = \overline{0,n}; \; \lambda \geq 1 \tag{4}$$

Here we emphasize that the smaller the δ value (or the greater λ value), the closer the endpoints of the integration of the double interpolant curve $\tilde{k}_{n,n}(x)$ to the exact curve of the integral values $\tilde{k}(x)$ at the endpoints of the domain of integration. Moreover, the value of λ depends on the length $(b-a)$ which we usually take it by the inequality $5 \leq \lambda \leq 10$ for $(b-a)=1$. Based on $\{x_i\}_{i=0}^{n}$ we construct the barycentric functions $\tau_i(x)$, by which we present the known square Maclaurin Coefficients matrix $\mathrm{A}^T = \left[a_{ij}\right]_{i,j=0}^{n}$ whose entries a_{ij} are then defined by

$$a_{ij}=\frac{\tau_i^{(j)}(0)}{j!};\tau_i(x)=\frac{\varsigma_i(x)}{\varphi(x)};\varphi(x)=\sum_{i=0}^{n}w_i\varsigma_i(x),\varsigma_i(x)=\frac{1}{x-x_i} \tag{5}$$

Thus, we get, similar to (6), the Maclaurin barycentric matrix-vector interpolant polynomial $k_n(x_i,t)$ of the n^{th} degree through the four matrices in the form

$$k_n(x_i,t)=\mathrm{X}(x)\,\mathrm{AWK}(x_i,t) \tag{6}$$

where, the column matrix $\mathrm{K}(x_i,t)=\left[k(x_i,t)\right]_{i=0}^{n}$ of the order $(n+1)\times n$ is defined by

$$\mathrm{K}^T(x_i,t)=\left[k(x_0,t)\;\; k(x_1,t)\;\; ...\;\; k(x_n,t)\right];n\geq 1 \tag{7}$$

Now, it is required to interpolate each entry $k(x_i,t)$ with respect to the variable t to complete the interpolation prosses. How will we choose the nodes which corresponding to the variable t? We will choose n+1 nodes , denoted by $\left\{t_j^i\right\}_{j=0}^{n}$ to each node x_i such that $x_i-t_j^i>0$; $j=\overline{0,n}$; this will be valid for each $i=0,1,2,...,n$. For example, the set of nodes for the variable t that is assigned to the node x_0 will be denoted by $\left\{t_j^0\right\}_{j=0}^{n}$, for the node x_1 will be denoted by $\left\{t_j^1\right\}_{j=0}^{n}$, and for x_n will be denoted by $\left\{t_j^n\right\}_{j=0}^{n}$ and so on. Furthermore, to interpolate each entry $k(x_i,t)$ we first construct the n+1 barycentric functions $\mu_j^i(t)$ for each $i=\overline{0,n}$ which is associated to each set of $(n+1)$ nodes $\left\{t_j^i\right\}_{j=0}^{n}$ for all $i=\overline{0,n}$. Second, for each barycentric function of $\mu_j^i(t)$,we create the corresponding Maclaurin coefficients square matrix denoted by $\mathrm{E}_i=\left[\nu_{jq}^i\right]_{j,q=0}^{n}$; $i=\overline{0,n}$. The entries ν_{jq}^i are defined by

$$\nu_{jq}^i=\frac{\left(\mu_j^i(t)\right)^{(q)}(0)}{q!}\;;j,q=\overline{0,n}\;\;\forall i=0,n \tag{8}$$

wherever,

$$\mu_j^i(t)=\frac{\xi_j^i(t)}{\bar{\phi}_i(x)},\bar{\phi}_i(t)=\sum_{j=0}^{n}w_j\xi_j^i(t),\xi_j^i(t)=\frac{1}{t-t_j^i};j=\overline{0,n}\;\forall i=0,n \tag{9}$$

Thus, for all the $(n+1)$ nodes $\{x_i\}_{i=0}^{n}$, we have a square matrix $\mathrm{T}=\left[t_j^i\right]_{i,j=0}^{n}$. All the sets of nodes t_j^i must fall within the domain $[a,b]$ and never outside, besides emphasizing that the integrand kernel never become singular when $x_i \to t_j^i$. The likelier way to achieve this goal is to choose t_j^i by the following rule

$$t_j^i=\frac{j\left(x_i+b\right)}{2n}\ ;\ j=\overline{0,n}\ \forall\ i=\overline{0,n} \tag{10}$$

Consequently, we get each entry $k\left(x_i,t\right)$ where $i=\overline{0,n}$ of the column matrix $\mathrm{K}\left(x_i,t\right)$ in terms of $t_j^i;\ j=\overline{0,n}\ \forall\ i=\overline{0,n}$ as follows

$$k\left(x_i,t\right)=k\left(x_i,\left\{t_j^i\right\}_{j=0}^{n}\right)=\mathrm{X}\left(t\right)\mathrm{E}_i^T\mathrm{WN}\ \forall\ i=\overline{0,n} \tag{11}$$

where $\mathrm{X}\left(t\right)=\left[t^i\right]_{i=0}^{n}$ is $1\times(n+1)$ monomial basis functions row matrix and the $(n+1)\times n$ column matrix N is defined by

$$\mathrm{N}=\left[n_i\right]_{i=0}^{n};n_i=k\left(x_i,t_j^i\right)\forall\ j=\overline{0,n} \tag{12}$$

Finally, by inversing the matrix multiplication of (11), we get

$$k\left(x_i,t\right)=\mathrm{N}^T\mathrm{WE}_i\mathrm{X}^T\left(t\right)\ \forall\ i=\overline{0,n} \tag{13}$$

Since

$$\mathrm{N}^T=\left[k\left(x_j,t_j^i\right)\ \ k\left(x_j,t_j^i\right)\ \ \ldots\ \ k\left(x_j,t_j^i\right)\right]_{j=0}^{n}\ \forall\ i=\overline{0,n} \tag{14}$$

Then, we find that

$$\mathrm{N}^T\mathrm{WE}_i=\sum_{j=0}^{n}\gamma_{ij}\ \forall\ i=\overline{0,n} \tag{15}$$

In matrix form upon considering the $n-$power series $\sum_{j=0}^{n}\gamma_{ij}\forall\ i=\overline{0,n}$, (15) can be rewritten in the form

$$\mathrm{N}^T\mathrm{WE}_i=\Omega;\ \Omega=\left[\gamma_{ij}\right]_{i,j=0}^{n}\ \forall\ i=\overline{0,n} \tag{16}$$

By substituting (16) into (13), we get the matrix-vector double barycentric interpolant kernel $k_{n,n}(x,t)$ in the matrix form

$$k_{n,n}(x,t)=\mathrm{X}(x)\,\mathrm{AW}\Omega\mathrm{X}^{T}(t) \tag{17}$$

The integration of $k_{n,n}(x,t)$ with respect to t is denoted by $\tilde{k}_{n,n}(x)$ and is given by

$$\tilde{k}_{n,n}(x)=\mathrm{X}(x)\,\mathrm{AW}\Omega\Phi\mathrm{M} \tag{18}$$

where M is the column matrix of order $(n+1)\times 1$ such that $\mathrm{M}=\left[\frac{1}{i+1}\left(b^{i+1}-a^{i+1}\right)\right]_{i=0}^{n}$. The matrix-vector barycentric double interpolant kernel $k_{n,n}(x,t)$ given by (17) and its integration denoted by $\tilde{k}_{n,n}(x)$ that was given by (18) based on the node's distribution (4) and (10) we refer to it with the phrase "Rule (I)".

To obtain Rule (II), we provide other nodes distributions for the variables x,t. Let

$$x_i=(a+\delta_1)+ih\ ;h=(b-a-2\delta_1)/n\ ;\delta_1\geq 0, i=\overline{0,n} \tag{19}$$

and

$$t_j^i=3/(5n)+abs\left(j\left(x_i-\delta_2\right)/n\right);\delta_2=(n+1)/(n+2);\ j=\overline{0,n}\ \forall\ i=\overline{0,n} \tag{20}$$

Hence the Maclaurin barycentric matrix-vector double interpolant kernel $k_{n,n}(x,t)$ given by (17) and the integration of which that was given by (18) based on the node's distribution (19) and (20) we refer to it with the phrase "Rule (II)".

To obtain Rule (III), we provide different nodes distributions for the variables x,t. Let

$$x_i=(a+\delta_1)+ih;h=\left((b-\delta_1)-(a+\delta_1)\right)/n,\delta_1=1/5n \tag{21}$$

and

$$t_j^i=a+j\left|\left(x_i-\delta_2\right)\right|/(n+1),\delta_2=\frac{n}{n+1};\ j=\overline{0,n}\ \forall\ i=\overline{0,n} \tag{22}$$

Hence the matrix-vector double barycentric interpolant kernel $k_{n,n}(x,t)$ given by (17) and the integration of which that was given by (18) based on the new node's distribution (21) and (22) we refer to it with the phrase "Rule (III)".

3. COMPUTATIONAL RESULTS

We designed 3-codes using MATLAB, R2019a for the computation of the double interpolant kernel integration $\tilde{k}_{2,2}(x)$ subjected to the weakly singular kernels of the Fredholm integral equation of the second kind. We have solved four examples in detail. For examples 1 and 2, we apply the rules (I), (II). For examples 3 and 4, we apply rule (III).

Example 1

Given the singular kernels $k^{\alpha}(x,t)=|x-t|^{-\alpha}$; $0\le x,t\le 1$ for $\alpha=1/2,1/4,1/3,1/5$, we first find the Maclaurin barycentric Lagrange double interpolant polynomials $k_{n,n}^{\alpha}(x,t)$ and hence integrate them to find the double interpolant integrals denoted by $\tilde{k}_{n,n}^{\alpha}(x)=\int_0^1 k_{n,n}^{\alpha}(x,t)\,dt$. The obtained double interpolant integral kernels $\tilde{k}_{n,n}^{\alpha}(x)$ will be compared with the exact (if exists) or with the numerical integral values denoted by $\tilde{k}^{\alpha}(x_i)=\int_0^1 k^{\alpha}(x_i,t)\,dt$ at $x=0.0:0.1:1.0$. By applying Formula (I) with $\lambda=5$ for $\alpha=1/2,1/4,1/3,2/5$, the equidistance nodes distributions $\{x_i\}_{i=0}^{n}$ and $\left\{t_j^i\right\}_{i,j=0}^{n}$ that correspond to the two variables x and t respectively, are common for all $\alpha=1/2,1/4,1/3,2/5$ and are given by

$$\{x_i\}_{i=0}^{2}=\{1/15,1/2,14/15\},\left[t_j^i\right]_{i,j=0}^{2}{}^{2}_{i,j=0}=\begin{bmatrix}0 & 4/15 & 8/15\\ 0 & 3/8 & 3/4\\ 0 & 29/60 & 29/30\end{bmatrix} \tag{23}$$

Based on (23), we find the double interpolant kernels $k_{n,n}^{\alpha}(x,t)$ and the associated double interpolant integrals $\tilde{k}_{n,n}^{\alpha}(x)$ for $\alpha=1/2,1/4,1/3,2/5$ as follows

$$k_{2,2}^{1/2}(x,t)=5.5375x^2-8.812x-t\left(63.886x^2-69.712x+12.123\right)+4.4358 \tag{24}$$
$$+t^2\left(78.776x^2-77.071x+10.868\right),\ \tilde{k}_{2,2}^{1/2}(x)=-0.14657x^2+0.3536x+1.9968$$

$$k_{2,2}^{1/4}(x,t)=1.6162x^2-t\left(19.448x^2-21.291x+3.4564\right)-2.713x+2.1417 \quad (25)$$
$$+t^2\left(23.118x^2-22.375x+2.7051\right),\ \tilde{k}_{2,2}^{1/4}(x)=-0.40203x^2+0.47429x+1.3152$$

$$k_{2,2}^{1/3}(x,t)=2.5819x^2-t\left(30.557x^2-33.413x+5.5567\right)-4.2468x+2.7379 \quad (26)$$
$$+t^2\left(36.773x^2-35.74x+4.5781\right),\ \tilde{k}_{2,2}^{1/3}(x)=-0.43924x^2+0.54649x+1.4856$$

$$k_{2,2}^{1/5}(x,t)=t^2\left(15.78x^2-14.756x+1.4302\right)-1.8598x+1.0867x^2+1.8069 \quad (27)$$
$$-t\left(13.607x^2-14.641x+2.1892\right),\ \tilde{k}_{2,2}^{1/5}(x)=-0.45702x^2+0.54243x+1.1891$$

By applying formula (II) with $\delta_1=0.1$ for $\alpha=1/2.1/4,1/5$ and $\delta_1=1/13$ for $\alpha=1/5$, the equidistance nodes distributions $\{x_i\}_{i=0}^{n}$ and $\left\{t_j^i\right\}_{i,j=0}^{n}$ that correspond to the two variables x and t respectively, are common for all $\alpha=1/2,1/4,1/3,2/5$ and are given by

$$\{x_i\}_{i=0}^{2}=\{1/10,1/2,9/10\},\left[t_j^i\right]_{i,j=0}^{2}=\begin{bmatrix}3/10 & 5/8 & 19/20\\ 3/10 & 17/40 & 11/20\\ 3/10 & 3/8 & 9/20\end{bmatrix} \quad (28)$$

Based on (28), we find the double interpolant polynomials $k_{n,n}^{\alpha}(x,t)$ and the associated interpolant integrals $\tilde{k}_{n,n}^{\alpha}(x)$ for $\alpha=1/2,1/4,1/3,2/5$ as follows

$$k_{2,2}^{1/2}(x,t)=t^2\left(133.2x^2-134.13x+14.734\right)-39.992x+37.024x^2+7.1526 \quad (29)$$
$$-t\left(173.22x^2-179.45x+21.301\right),\ \tilde{k}_{2,2}^{1/2}(x)=-5.1848x^2+5.0236x+1.4136$$

$$k_{2,2}^{1/4}(x,t)=11.708x^2-t\left(56.93x^2-59.262x+7.1631\right)+3.1236-12.832x \quad (30)$$
$$+t^2\left(47.213x^2-47.478x+5.162\right),\tilde{k}_{2,2}^{1/4}(x)=-1.0198x^2+0.97271x+1.2627$$

$$k_{2,2}^{1/3}(x,t)=t^2\left(71.029x^2-71.458x+7.7915\right)-19.869x+18.226x^2+4.2031 \quad (31)$$
$$-t\left(87.524x^2-90.946x+10.921\right),\ \tilde{k}_{2,2}^{1/3}(x)=-1.8597x^2+1.7842x+1.3398$$

$$k_{2,2}^{1/5}(x,t)=t^2(35.047x^2-35.235x+3.8248)-9.3778x+8.526x^2+2.578 \quad (32)$$
$$-t(41.769x^2-43.531x+5.2834),\ \tilde{k}_{2,2}^{1/5}(x)=-0.67622x^2+0.64259x+1.2112$$

Tables 1,2,3, and 4 show the numerical integral values $\tilde{k}^{\alpha}(x_i)$, the double interpolant integral values $\tilde{k}_{2,2}^{\alpha}(x_i)$ and the absolute errors $\tilde{R}_{n,n}^{\alpha}(x_i)=\left|\tilde{k}^{\alpha}(x_i)-\tilde{k}_{n,n}^{\alpha}(x_i)\right|$ at the points $x_i=0.0{:}0.1{:}1.0$ according to formulas (I) and (II) for $\alpha=1/2,1/4,1/3,2/5$. In figures 1,2.3 and 4, plotted are the graphs of the numerical integral values $\tilde{k}^{\alpha}(x_i)$ and the double interpolant integral values $\tilde{k}_{n,n}^{\alpha}(x_i)$ at the points $x_i=0.0{:}0.1{:}0.9$ for $\alpha=1/2$ because the integral diverges for $x=1$, and at the points $x_i=0.0{:}0.1{:}1.0$ for $\alpha=1/4,1/3,2/5$. From table 1, we find that the kernel value $k(0,0)$ for $\alpha=1/4,1/3,2/5$ does not exist while by the Rules (I) and (II), we get the values $k_{2,2}^{1/2}(0,0)=4.4358$ and $k_{2,2}^{1/2}(0,0)=7.1526$. For $\alpha=1/4$, we obtain $k_{2,2}^{1/4}(0,0)=2.1417$ and $k_{2,2}^{1/4}(0,0)=3.1236$. For $\alpha=1/3$, we obtain $k_{2,2}^{1/3}(0,0)=2.7379$ and $k_{2,2}^{1/3}(0,0)=4.2031$. For $\alpha=1/5$, we get $k_{2,2}^{1/5}(0,0)=1.8069$ and $k_{2,2}^{1/5}(0,0)=2.578$. Besides, the numerical integral value $\tilde{k}^{1/2}(1)$ does not exist whereas by Rule (I), we obtain $\tilde{k}_{2,2}^{1/2}(1)=2.2038$ and by Rule (II), we get $\tilde{k}_{2,2}^{1/2}(1)=1.2524$.

Example 2

Consider the weakly singular Fredholm integral equation of the second kind

$$\frac{3\sqrt{2}}{4}\varphi(x)-\int_0^1\frac{\varphi(t)}{\sqrt{|x-t|}}dt=3\left(x(1-x)\right)^{\frac{3}{4}}-\frac{3\pi}{8}\left(1+4x(1-x)\right)^{\frac{3}{4}} \quad (33)$$

whose exact solution [19] is given by $\varphi(x)=2\sqrt{2}\left(x(1-x)\right)^{\frac{3}{4}}$. Substituting $\varphi(x)$ into (33), we get the singular kernel $\vartheta(x,t)=\dfrac{\left(t(1-t)\right)^{\frac{3}{4}}}{\sqrt{|x-t|}}$ such that

$$\tilde{\vartheta}(x)=\int_0^1\vartheta(x,t)dt=\int_0^1\frac{\left(t(1-t)\right)^{\frac{3}{4}}}{\sqrt{|x-t|}}dt=\frac{3\pi}{16\sqrt{2}}\left(1+4x(1-x)\right)^{\frac{3}{4}} \quad (34)$$

This integral is singular due to the discontinuity of the integrand kernel when $x=t=0$ and generally when $x\to t$. By using the Formula (I) with $\delta_1=1/15$, we find $\vartheta^{\mathrm{I}}_{2,2}(x,t)$ and $\tilde{\vartheta}^{\mathrm{I}}_{2,2}(x)$ as follows

$$\begin{aligned}\vartheta^{\mathrm{I}}_{2,2}(x,t)&=\left(-t(t-1)\right)^{(3/4)}\left(5.5375x^2-8.812x+4.4358\right)\\&-t\left(63.886x^2-69.712x+12.123\right)\left(-t(t-1)\right)^{(3/4)}\\&+t^2\left(-t(t-1)\right)^{(3/4)}\left(78.776x^2-77.071x+10.868\right)\end{aligned}\tag{35}$$

And

$$\tilde{\vartheta}^{\mathrm{I}}_{2,2}(x)=-0.59341x^2+0.63399x+0.4308\tag{36}$$

Using the Rule (II) with $\delta_1=0.1$, we get

$$\begin{aligned}\tilde{\vartheta}^{\mathrm{II}}_{2,2}(x,t)&=\left(-t(t-1)\right)^{(3/4)}\left(37.024x^2-39.992x+7.1526\right)\\&-t\left(-t(t-1)\right)^{(3/4)}\left(173.22x^2-179.45x+21.301\right)\\&+t^2\left(-t(t-1)\right)^{(3/4)}\left(133.2x^2-134.13x+14.734\right)\end{aligned}\tag{37}$$

And

$$\tilde{\vartheta}^{\mathrm{II}}_{2,2}(x)=-2.2582x^2+2.2238x+0.25526\tag{38}$$

In tables 5, given are the exact integral values $\tilde{\vartheta}(x_i)$, the double interpolant integral values $\tilde{\vartheta}^{\mathrm{I}}_{2,2}(x)$ and $\tilde{\vartheta}^{\mathrm{II}}_{2,2}(x)$ according to the Rules (I) and (II), and the absolute errors $\tilde{R}^{s}_{2,2}(x_i)=\left|\tilde{\vartheta}(x_i)-\tilde{\vartheta}^{s}_{2,2}(x_i)\right|$ at the points $x_i=0.0{:}0.1{:}1.0$, where $s=\mathrm{I,II}$ denotes Rule (I) and Rule (II). In figures 5, plotted are the graphs of the exact integral values $\tilde{\vartheta}(x_i)$ and the double interpolated integral values $\tilde{\vartheta}^{\mathrm{I}}_{2,2}(x_i)$ and $\tilde{\vartheta}^{\mathrm{II}}_{2,2}(x_i)$ at the points $x_i=0.0{:}0.1{:}1.0$. It is observed that the integrand kernel $\vartheta(x,t)$ is undefined at $x=t=0$ whereas the double interpolated kernel give $\vartheta^{\mathrm{I}}_{2,2}(0,0)=\vartheta^{\mathrm{II}}_{2,2}(0,0)=0$.

Example 3

Consider the weakly singular Fredholm integral equation of the second kind

$$\phi(x)-\frac{2}{3}\int_{-1}^{1}\frac{1}{\sqrt{|x-t|}}\phi(x)\,dt=\left(1-x^2\right)^{\frac{3}{4}}-\frac{\pi}{2\sqrt{2}}\left(2-x^2\right) \tag{39}$$

whose exact solution [20] is given by $\phi(x)=\left(1-x^2\right)^{\frac{3}{4}}$. Substituting $\phi(x)$ into (39), we get the singular kernel $K(x,t)=\dfrac{\left(1-t^2\right)^{\frac{3}{4}}}{\sqrt{|x-t|}}$ such that

$$\tilde{K}(x)=\int_{-1}^{1}K(x,t)dt=\int_{-1}^{1}\frac{\left(1-t^2\right)^{\frac{3}{4}}}{\sqrt{|x-t|}}dt=\frac{3\pi}{4\sqrt{2}}\left(2-x^2\right) \tag{40}$$

This integral is singular due to the discontinuity of the integrand kernel when $x=t=0$ and generally when $x\to t$. By using Rule (III), we find the set of $x-$nodes distribution $\{x_i\}_{i=0}^{2}$ and the matrix of $t-$nodes distributions as follows

$$\{x_i\}_{i=0}^{2}=\{-0.9,0,0.9\},\left[t_j^i\right]_{i,j=0}^{2}=\begin{bmatrix}-1 & -43/90 & 2/45\\ -1 & -7/9 & -5/9\\ -1 & -83/90 & -38/45\end{bmatrix} \tag{41}$$

The double interpolant kernel $K_{22,2}^{\mathrm{III}}(x,t)$ that interpolate $K(x,t)$ and the integration of $K_{22}^{\mathrm{III}}(x,t)$ denoted by $\tilde{K}_{22}^{\mathrm{III}}(x)$ are given by

$$\begin{aligned}K_{22}^{\mathrm{III}}(x,t)&=t^2\left(1-t^2\right)^{(3/4)}\left(0.38854x^2-1.0875x+0.74777\right)\\&-\left(1-t^2\right)^{(3/4)}\left(1.4441x^2+0.016296x-2.1841\right)\\&+t\left(1-t^2\right)^{(3/4)}\left(-2.2209x^2+0.25003x+1.9319\right)\end{aligned} \tag{42}$$

$$\tilde{K}_{22}^{\mathrm{III}}(x)=-1.9522x^2-0.37088x+3.3792 \tag{43}$$

In tables 6, given are the exact integral values $\tilde{K}(x_i)$, the double interpolant integral values $\tilde{K}_{22}^{\mathrm{III}}(x_i)$, and the absolute errors $\tilde{R}_{2,2}^{\mathrm{III}}(x_i)=\left|\tilde{K}(x_i)-\tilde{K}_{2,2}^{\mathrm{III}}(x_i)\right|$ at the points $x_i=0.0{:}0.1{:}1.0$. In

figures 6, plotted are the graphs of the exact integral values $\tilde{K}(x_i)$ and the double interpolate integral values $\tilde{K}_{22}^{\mathrm{III}}(x_i)$ at the points $x_i=0.0:0.1:1.0$. It is observed that the integrand kernel $K(x,t)$ is undefined at $x=t=0$ whereas we get $K_{22}^{\mathrm{III}}(0,0)=0$.

Example 4

Consider the weakly singular Fredholm integral equation of the second kind

$$\tau(x)-\int_{-1}^{1}\log|x-t|\,\tau(t)dt=x-0.5\left[x^2\log(x)+\left(1-x^2\right)\log(1-x)-x-0.5\right] \tag{44}$$

whose exact solution [20] is given by $\tau(x)=x$. Substituting $\tau(x)$ into (44.), we get the singular kernel $\Psi(x,t)=t\times\log|x-t|$. The integration of this kernel is denoted by $\tilde{\Psi}(x)$. Thus, we have

$$\tilde{\Psi}(x)=\int_{-1}^{1}\Psi(x,t)\,dt=\int_{-1}^{1}t\log|x-t|dt=0.5\left[x^2\log(x)+\left(1-x^2\right)\log(1-x)-x-0.5\right] \tag{45}$$

This integral is singular due to the discontinuity of the integrand kernel at $x=t=0$ and generally when $x\to t$. By using Rule (III), with some change in the rule of the nodes t_j^i to become

$$t_j^i=(n+1)/(n+3)+j\left|\left(x_i-\delta_2\right)\right|/(n),\delta_2=\frac{n}{n+1};\ j=\overline{0,n}\ \forall\ i=\overline{0,n} \tag{46}$$

we find the set of $x-$nodes distribution $\{x_i\}_{i=0}^{2}$ and the matrix of the $t-$nodes distributions as follows

$$\{x_i\}_{i=0}^{2}=\{-0.9,0,0.9\},\left[t_j^i\right]_{i,j=0}^{2}=\begin{bmatrix}3/5 & -11/60 & 29/30\\ 3/5 & 4/15 & -1/15\\ 3/5 & 43/60 & 5/6\end{bmatrix}. \tag{47}$$

Hence, we get $\Psi_{22,2}^{\mathrm{III}}(x,t)$ and $\tilde{\Psi}_{22}^{\mathrm{III}}(x)$ by

$$\Psi_{22}^{\mathrm{III}}(x,t)=t^2\left(8.0447x^2+10.772x+4.6767\right)-t\left(1.3058x^2+3.8098x+2.3848\right) \tag{48}$$
$$-t^3\left(9.3981x^2+9.8536x+2.5891\right).$$

And

$$\tilde{\Psi}_{22}^{\mathrm{III}}(x)=-0.32084x^2-0.77777x-0.28076 \tag{49}$$

Table 7 shows the exact integral values $\tilde{\Psi}(x_i)$, the double interpolant integral values $\tilde{\Psi}_{22}^{\mathrm{III}}(x_i)$ and the absolute errors $\tilde{R}_{2,2}^{\mathrm{III}}(x_i)=\left|\tilde{\Psi}(x_i)-\tilde{\Psi}_{2,2}^{\mathrm{III}}(x_i)\right|$ at the points $x_i=0.0{:}0.1{:}1.0$. In figure 7, plotted are the graphs of the exact integral values $\tilde{\Psi}(x_i)$ and the double interpolate integral values $\tilde{\Psi}_{22}^{\mathrm{III}}(x_i)$ at the points $x_i=0.0{:}0.1{:}1.0$. It is observed that the integrand kernel $K(x,t)$ is undefined at $x=t=0$, whereas the double interpolant kernel gives $\Psi_{22}^{\mathrm{III}}(0,0)=0$.

4. TABLES

Table 1

A comparison of the numerical Integral Values $\tilde{k}^{1/2}(x_i)$ with the double interpolant integral values $\tilde{k}_{2,2}^{1/2}(x_i)$ obtained by using Rules (I) and (II).

Rule (I)				Rule (II)			
x_i	$\tilde{k}^{1/2}(x_i)$	$\tilde{k}_{2,2}^{1/2}(x_i)$	$\tilde{R}_{2,2}^{1/2}$	x_i	$\tilde{k}^{1/2}(x_i)$	$\tilde{k}_{2,2}^{1/2}(x_i)$	$\tilde{R}_{2,2}^{1/2}$
0	2	1.9968	0.0032	0	2	1.4136	0.5864
0.1	2.5298	2.0307	0.4991	0.1	2.5298	1.8641	0.6657
0.2	2.6833	2.0617	0.6216	0.2	2.6833	2.2109	0.4724
0.3	2.7688	2.0897	0.6791	0.3	2.7688	2.454	0.3148
0.4	2.8141	2.1148	0.6993	0.4	2.8141	2.5935	0.2206
0.5	2.8284	2.137	0.6914	0.5	2.8284	2.6292	0.1992
0.6	2.8141	2.1562	0.6579	0.6	2.8141	2.5612	0.2529
0.7	2.7688	2.1725	0.5963	0.7	2.7688	2.3896	0.3792
0.8	2.6833	2.1859	0.4974	0.8	2.6833	2.1142	0.5691
0.9	2.5298	2.1963	0.3335	0.9	2.5298	1.7352	0.7946
1	NaN	2.2038	***	1	NaN	1.2524	***

Table 2

A comparison of the numerical Integral Values $\tilde{k}^{1/4}(x_i)$ with the double interpolant integral values $\tilde{k}_{2,2}^{1/4}(x_i)$ obtained by using Rules (I) and (II).

Rule (I)				Rule (II)			
x_i	$\tilde{k}^{1/4}(x_i)$	$\tilde{k}_{2,2}^{1/4}(x_i)$	$\tilde{R}_{2,2}^{1/4}$	x_i	$\tilde{k}^{1/4}(x_i)$	$\tilde{k}_{2,2}^{1/4}(x_i)$	$\tilde{R}_{2,2}^{1/4}$
0	1.3333	1.3152	0.0181	0	1.3333	1.2627	0.0706
0.1	1.4691	1.3586	0.1105	0.1	1.4691	1.3498	0.1193
0.2	1.5266	1.394	0.1326	0.2	1.5266	1.4165	0.1101
0.3	1.5609	1.4213	0.1396	0.3	1.5609	1.4627	0.0982
0.4	1.5796	1.4406	0.139	0.4	1.5796	1.4886	0.091
0.5	1.5856	1.4518	0.1338	0.5	1.5856	1.4941	0.0915
0.6	1.5796	1.455	0.1246	0.6	1.5796	1.4792	0.1004
0.7	1.5609	1.4502	0.1107	0.7	1.5609	1.4439	0.117
0.8	1.5266	1.4373	0.0893	0.8	1.5266	1.3882	0.1384
0.9	1.4691	1.4164	0.0527	0.9	1.4691	1.3121	0.157
1	1.3333	1.3875	0.0542	1	1.3333	1.2156	0.1177

Table 3

A comparison of the numerical Integral Values $\tilde{k}^{1/3}(x_i)$ with the double interpolant integral values $\tilde{k}_{2,2}^{1/3}(x_i)$ obtained by using Rules (I) and (II).

Rule (I)				Rule (II)			
x_i	$\tilde{k}^{1/3}(x_i)$	$\tilde{k}_{2,2}^{1/3}(x)$	$\tilde{R}_{2,2}^{1/3}$	x_i	$\tilde{k}^{1/3}(x_i)$	$\tilde{k}_{2,2}^{1/3}(x_i)$	$\tilde{R}_{2,2}^{1/3}$
0	1.5	1.4856	0.0144	0	1.5	1.3398	0.1602
0.1	1.7214	1.5358	0.1856	0.1	1.7214	1.4996	0.2218
0.2	1.8057	1.5773	0.2284	0.2	1.8057	1.6222	0.1835
0.3	1.8548	1.61	0.2448	0.3	1.8548	1.7077	0.1471
0.4	1.8814	1.6339	0.2475	0.4	1.8814	1.7559	0.1255
0.5	1.8899	1.649	0.2409	0.5	1.8899	1.767	0.1229
0.6	1.8814	1.6553	0.2261	0.6	1.8814	1.7408	0.1406
0.7	1.8548	1.6529	0.2019	0.7	1.8548	1.6775	0.1773
0.8	1.8057	1.6416	0.1641	0.8	1.8057	1.577	0.2287
0.9	1.7214	1.6216	0.0998	0.9	1.7214	1.4393	0.2821
1	1.5	1.5928	0.0928	1	1.5	1.2644	0.2356

Table 4

A comparison of the numerical Integral Values $\tilde{k}^{1/5}(x_i)$ with the double interpolant integral values $\tilde{k}_{2,2}^{1/5}(x_i)$ obtained by using Rules (I) and (II).

Rule (I)				Rule (II)			
x_i	$\tilde{k}^{1/5}(x_i)$	$\tilde{k}_{2,2}^{1/5}(x_i)$	$\tilde{R}_{2,2}^{1/5}$	x_i	$\tilde{k}^{1/5}(x_i)$	$\tilde{k}_{2,2}^{1/5}(x_i)$	$\tilde{R}_{2,2}^{1/5}$
0	1.25	1.1891	0.0609	0	1.25	1.2112	0.0388
0.1	1.3471	1.2387	0.1084	0.1	1.3471	1.2687	0.0784
0.2	1.3906	1.2793	0.1113	0.2	1.3906	1.3127	0.0779
0.3	1.4168	1.3106	0.1062	0.3	1.4168	1.3431	0.0737
0.4	1.4312	1.3329	0.0983	0.4	1.4312	1.3601	0.0711
0.5	1.4359	1.346	0.0899	0.5	1.4359	1.3635	0.0724
0.6	1.4312	1.35	0.0812	0.6	1.4312	1.3533	0.0779
0.7	1.4168	1.3448	0.072	0.7	1.4168	1.3297	0.0871
0.8	1.3906	1.3305	0.0601	0.8	1.3906	1.2925	0.0981
0.9	1.3471	1.3071	0.04	0.9	1.3471	1.2418	0.1053
1	1.25	1.2745	0.0245	1	1.25	1.1776	0.0724

Table 5

A comparison of the exact integral values $\tilde{k}(x)$ with the double interpolants integral values $\tilde{\mathcal{I}}_{2,2}^{\mathrm{I}}(x)$ and $\tilde{\mathcal{I}}_{2,2}^{\mathrm{II}}(x)$ for example 2 obtained by using Rules (I) and (II)

Rule (I)				Rule (II)			
x_i	$\tilde{k}(x)$	$\tilde{\mathcal{I}}_{2,2}^{\mathrm{I}}(x)$	$\tilde{R}_{2,2}^{\mathrm{I}}$	x_i	$\tilde{k}(x)$	$\tilde{\mathcal{I}}_{2,2}^{\mathrm{II}}(x)$	$\tilde{R}_{2,2}^{\mathrm{II}}$
0	0.41652	0.4308	0.01428	0	0.41652	0.25526	0.16126
0.1	0.52455	0.48826	0.03629	0.1	0.56647	0.45506	0.11141
0.2	0.60363	0.53386	0.06977	0.2	0.68309	0.60969	0.0734
0.3	0.65804	0.56759	0.09045	0.3	0.7664	0.71917	0.04723
0.4	0.68997	0.58945	0.10052	0.4	0.81638	0.78348	0.0329
0.5	0.7005	0.59944	0.10106	0.5	0.83304	0.80262	0.03042
0.6	0.68997	0.59756	0.09241	0.6	0.81638	0.7766	0.03978
0.7	0.65804	0.58382	0.07422	0.7	0.7664	0.70542	0.06098
0.8	0.60363	0.55821	0.04542	0.8	0.68309	0.58908	0.09401
0.9	0.52455	0.52073	0.00382	0.9	0.56647	0.42757	0.1389
1	0.41652	0.47138	0.05486	1	0.41652	0.22089	0.19563

Table 6

The exact integral values $\tilde{K}(x_i)$, the double interpolant integral values $\tilde{K}_{2,2}^{\mathrm{III}}(x)$, and the absolute errors $\tilde{R}_{2,2}^{\mathrm{III}}$ at $x_i = -1{:}0.1{:}1$

x_i	$\tilde{K}(x_i)$	$\tilde{K}_{2,2}^{\mathrm{III}}(x)$	$\tilde{R}_{2,2}^{\mathrm{III}}$
-1	1.6661	1.7979	0.1318
-0.9	1.9826	2.1317	0.1491
-0.8	2.2659	2.4265	0.1606
-0.7	2.5158	2.6822	0.1664
-0.6	2.7324	2.8989	0.1665
-0.5	2.9156	3.0766	0.161
-0.4	3.0656	3.2152	0.1496
-0.3	3.1822	3.3147	0.1325
-0.2	3.2655	3.3753	0.1098
-0.1	3.3155	3.3967	0.0812
0	3.3322	3.3792	0.047
0.1	3.3155	3.3226	0.0071
0.2	3.2655	3.2269	0.0386
0.3	3.1822	3.0922	0.09
0.4	3.0656	2.9185	0.1471
0.5	2.9156	2.7057	0.2099
0.6	2.7324	2.4539	0.2785
0.7	2.5158	2.163	0.3528
0.8	2.2659	1.8331	0.4328
0.9	1.9826	1.4641	0.5185
1	1.6661	1.0561	0.61

Table 7

The exact integral values $\tilde{\Psi}(x_i)$, the double interpolant integral values $\tilde{\Psi}_{2,2}^{\mathrm{III}}(x_i)$, and the absolute errors $\tilde{R}_{2,2}^{\mathrm{III}}$ at $x_i = -1{:}0.1{:}1$

x_i	$\tilde{\Psi}(x_i)$	$\tilde{\Psi}_{2,2}^{\mathrm{III}}(x)$	$\tilde{R}_{2,2}^{\mathrm{III}}$
-1	0.25	0.17617	0.07383
-0.9	0.21831	0.15935	0.05896
-0.8	0.1844	0.13611	0.04829
-0.7	0.14792	0.10646	0.04146
-0.6	0.10845	0.070395	0.038055
-0.5	0.065406	0.027911	0.037495
-0.4	0.018015	-0.02099	0.039005
-0.3	-0.0348	-0.07631	0.041505
-0.2	-0.09467	-0.13804	0.043366
-0.1	-0.16433	-0.20619	0.04186
0	-0.25	-0.28076	0.03076
0.1	-0.36367	-0.36175	0.00192
0.2	-0.4893	-0.44915	0.04015
0.3	-0.61647	-0.54297	0.0735
0.4	-0.73785	-0.6432	0.09465
0.5	-0.84657	-0.74985	0.09672
0.6	-0.93516	-0.86292	0.07224
0.7	-0.9944	-0.98241	0.01199
0.8	-1.0111	-1.1083	0.0972
0.9	-0.96142	-1.2406	0.27918
1	-0.75	-1.3794	0.6294

5. FIGURES

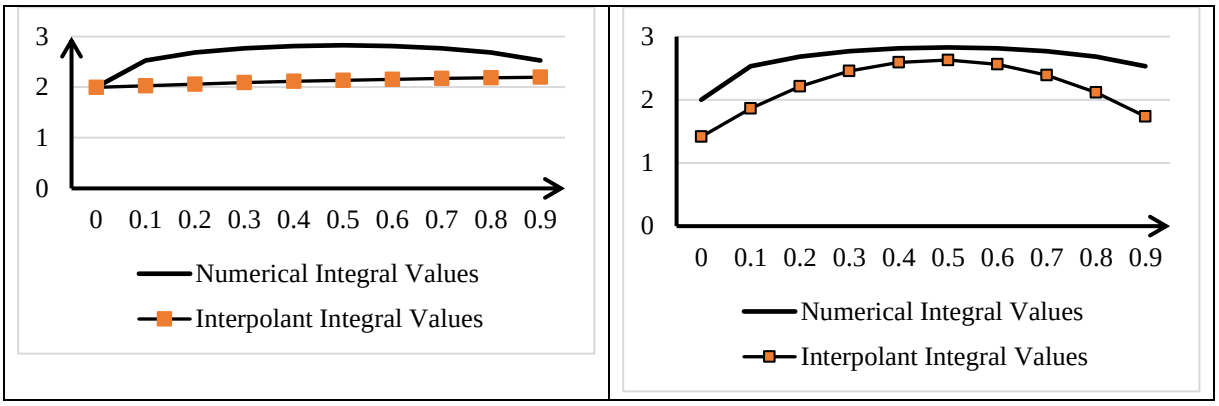

Fig. 1. A comparison of the graph of the numerical integral Values $\tilde{k}^{1/2}(x_i)$ with the graphs of the double interpolants integral values $\tilde{k}_{2,2}^{1/2}(x_i)$ by using Rules (I) and (II).

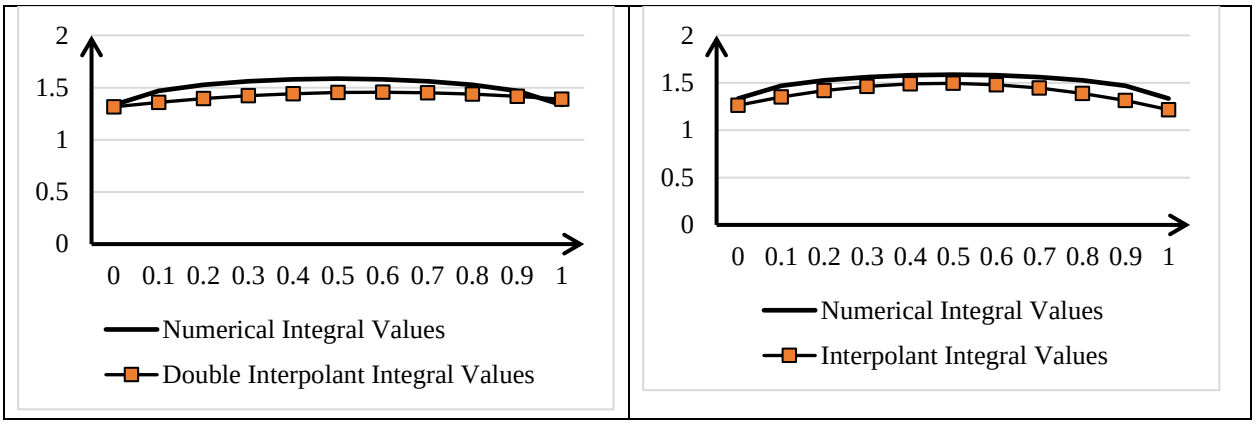

Fig. 2. A comparison of the graph of the numerical integral values $\tilde{k}^{1/4}(x_i)$ with the graphs of the double interpolants integral values $\tilde{k}_{2,2}^{1/4}(x_i)$ by using Rules (I) and (II)

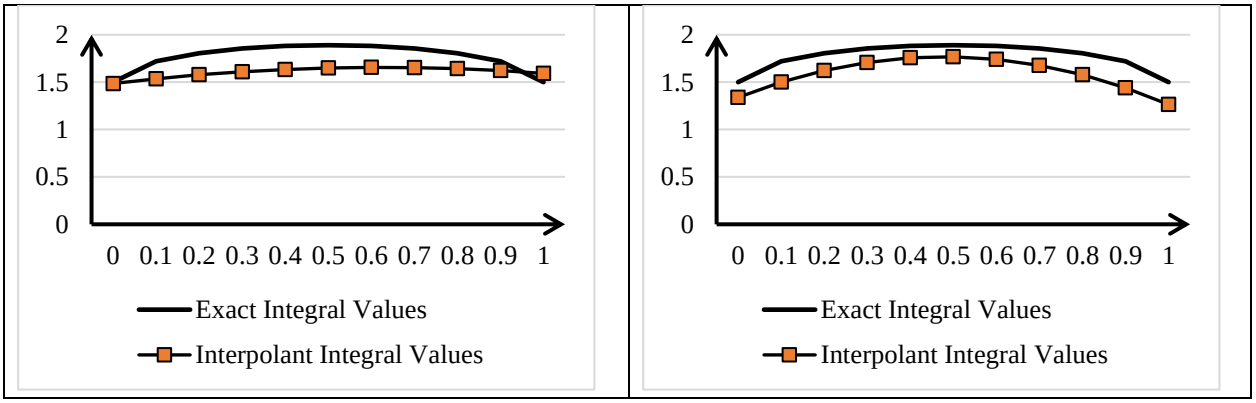

Fig. 3. A comparison of the graph of the numerical integral values $\tilde{k}^{1/3}(x_i)$ with the graphs of the double interpolants integral values $\tilde{k}_{2,2}^{1/3}(x_i)$ by using Rules (I) and (II)

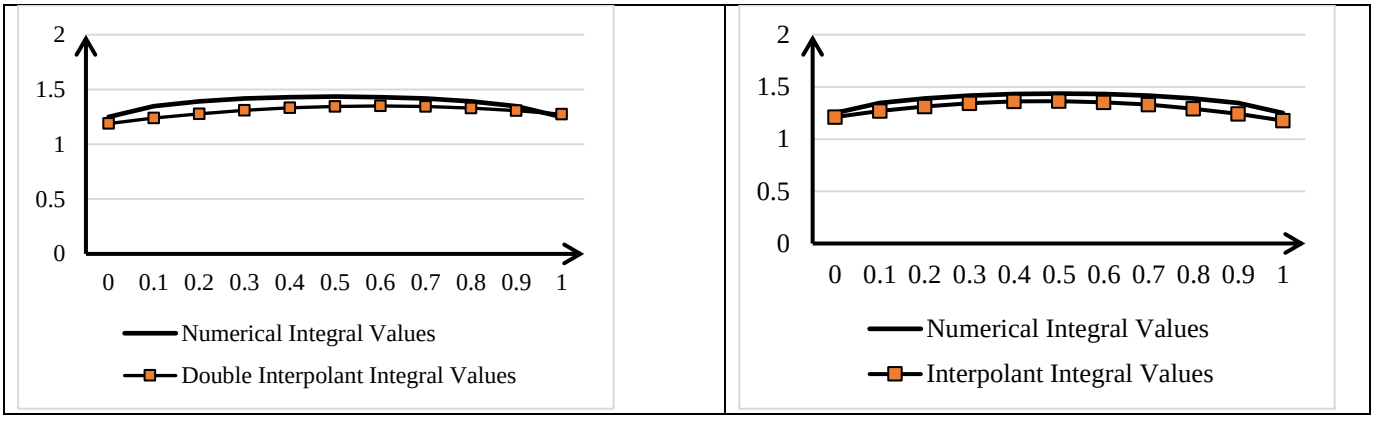

Fig. 4. A comparison of the graph of the numerical Integral Values $\tilde{k}^{1/5}(x_i)$ with the graphs of the double interpolants integral values $\tilde{k}_{2,2}^{1/5}(x_i)$ of Rules (I) and (II)

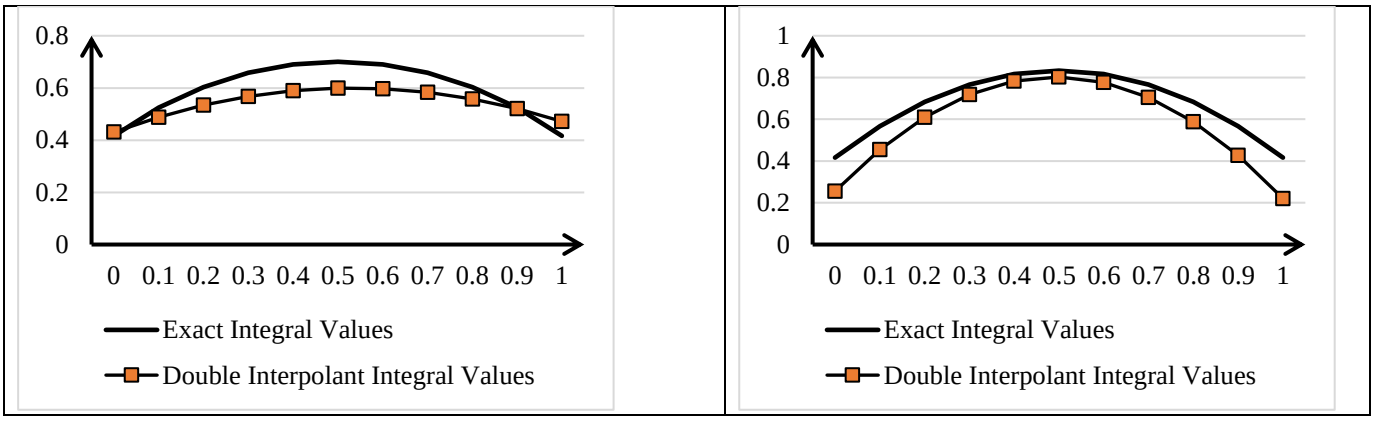

Fig. 5. A comparison of the graph of the numerical integral values $\tilde{k}(x_i)$ with the graphs of the double interpolants integral values $\tilde{k}_{2,2}(x_i)$ by using Rules (I) and (II).

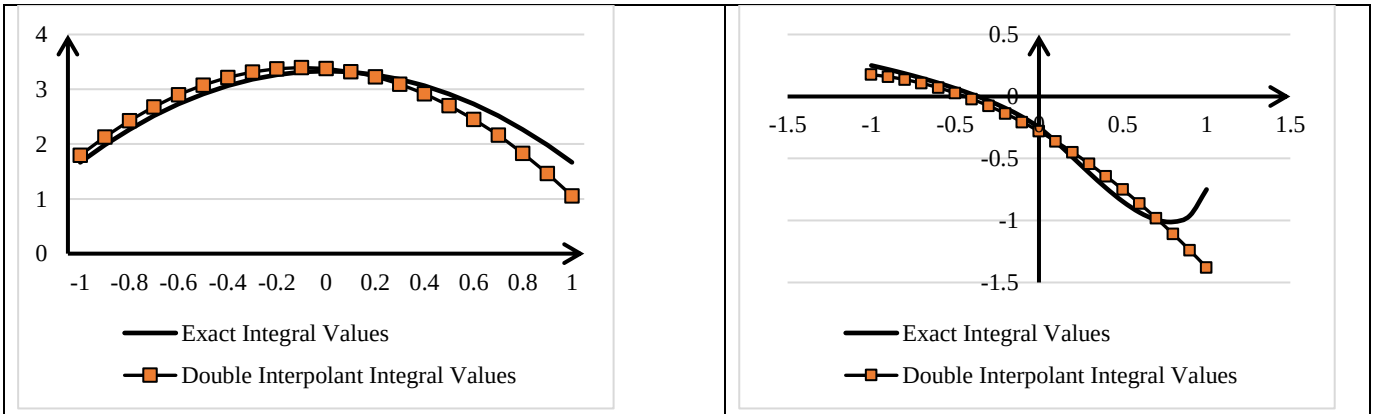

Fig. 6. The graphs of $\tilde{K}(x_i)$ and $\tilde{K}_{2,2}^{\mathrm{III}}(x_i)$ by using Rule (III

Fig. 7. The graphs of $\tilde{\Psi}(x_i)$ and $\tilde{\Psi}_{2,2}^{\mathrm{III}}(x_i)$ by using Rule (III)

6. CONCLUSION

In this paper, we presented a new interpolation method for solving different types of weakly singular kernels of the Fredholm integral equation of the second kind. We developed an advanced matrix-vector barycentric interpolation formula to find the matrix-vector double interpolant kernel free of any singularities via matrices, two of which are monomial basis functions of the two kernel variables. We achieved this procedure by creating three rules to ensure optimum distribution of the interpolation nodes within the domain of the integration domain and never become outside it. We defined the node distribution of the second variable of the singular kernel to be deepening on the node distribution of the first variable. We also define the node distribution for each variable as a function of the interpolant's degree and, at the same time, depend on some small real number greater than or equal to zero to ensure that the values under the square root of the kernel never become zero or negative. Four examples containing seven singular kernels were solved in detail and supplemented with tables and graphs. The obtained interpolate solutions by low-degree interpolants strongly converged to the exact (if existing) or to the numerical quadrature solutions. This confirms the originality of the newly presented method.

CONFLICT OF INTERESTS

The author(s) declare that there is no conflict of interests.

REFERENCES

[1] V. Jacquemet, Phase singularity detection through phase map interpolation: Theory, advantages and limitations, Computers Biol. Med. 102(1) (2018), 381-389.

[2] P.M. Barker and T.J. McDougall, Two interpolation methods using multiply rotated piecewise cubic hermite interpolating polynomials, J. Atmosph. Ocean. Technol. 37(4) (2020), 605–619.

[3] Y.L. Yeh, Vibration analysis of the plate with the regular and irregular domain by using the Barycentric Lagrange interpolation, J. Low Freq. Noise Vibrat. Active Control, 39(3) (2020), 485–501

[4] J. Liu, L.Y. Zhu, Bivariate Lagrange interpolation based on Chebyshev points of the second kind, Acta Math. Hungar. 159 (2019), 618–637.

[5] J.P. Berrut, L.N. Trefethen, Barycentric Lagrange interpolation, society for industrial and applied mathematics, SIAM Review, 46 (3) (2004), 501-517.

[6] N. J. Higham, The numerical stability of Barycentric Lagrange interpolation, IMA J. Numer. Anal. 24 (2004), 547-556.

[7] E. S. Shoukralla, B. M. Ahmed, The Barycentric Lagrange Interpolation via Maclaurin Polynomials for Solving the Second Kind Volterra Integral Equations, in: 2020 15th International Conference on Computer Engineering and Systems (ICCES), IEEE, Cairo, Egypt, 2020: pp. 1–6.

[8] E. S. Shoukralla, H. Elgohary, B. M. Ahmed, Barycentric Lagrange interpolation for solving Volterra integral equations of the second kind, J. Phys.: Conf. Ser. 1447 (2020), 012002.

[9] E. S. Shoukralla, B. M. Ahmed, Numerical Solutions of Volterra Integral Equations of the Second Kind using Lagrange interpolation via the Vandermonde matrix, J. Phys.: Conf. Ser. 1447 (2020) 012003.

[10] E. S. Shoukralla, B. M. Ahmed, Multi-techniques method for Solving Volterra Integral Equations of the Second Kind, in: 2019 14th International Conference on Computer Engineering and Systems (ICCES), IEEE, Cairo, Egypt, 2019: pp. 209–213.

[11] E. S. Shoukralla, B. M. Ahmed, Numerical Solutions of Volterra Integral Equations of the Second Kind Using Barycentric Lagrange with Chebyshev Interpolation, Menoufia J. Electron. Eng. Res. 28 (2019), 275–279.

[12] E. S. Shoukralla, M. A. Markos, The economized monic Chebyshev polynomials for solving weakly singular Fredholm integral equations of the first kind, Asian-European J. Math. 13 (2020), 2050030.

[13] E. S. Shoukralla and M. A. Markos, Numerical Solution of a Certain Class of Singular Fredholm Integral Equations of the First Kind via the Vandermonde Matrix, Int. J. Math. Models Meth. Appl. Sci. 14 (2020), 48-53.

[14] E. S. Shoukralla, M. Kamel, M. A. Markos, A New Computational Method for Solving Weakly Singular Fredholm Integral Equations of the First Kind, in: 2018 13th International Conference on Computer Engineering and Systems (ICCES), IEEE, Cairo, Egypt, 2018: pp. 202–207.

[15] J. Gao, A. Iserles, B. Gilvey, J. Trevelyan, Quadrature Methods for Highly Oscillatory Singular Integrals, J. Comput. Math. 39(2) (2021), 227-260.

[16] A. K. Lerner, A weak type estimate for rough singular integrals, European Mathematical Society, Rev. Mat. Iberoamer. 35 (2019), 1583–1602.

[17] B. Jaye, T. Merchán, Small local action of singular integrals on spaces of non-homogeneous type, Rev. Mat. Iberoam. 36 (2020), 2183–2207.

[18] A.K. Lerner, S. Ombrosi, I.P. Rivera-Ríos, Commutators of singular integrals revisited: commutators of singular integrals revisited, Bull. London Math. Soc. 51 (2019), 107–119.

[19] P. K. Kythe, P. Puri, Computational Methods for Linear Integral Equations, Birkhauser, Boston, 2002.

[20] B. L. Panigrahi, M. Mandal, G. Nelakanti, Legendre multi-Galerkin methods for Fredholm integral equations with weakly singular kernel and the corresponding eigenvalue problem, J. Comput. Appl. Math. 346 (2019), 224–236